Title: The type VI secretion system of *Sinorhizobium fredii* USDA257 is required for a successful symbiosis with *Glycine max* cv Pekin

Author list: Pedro José Reyes-Pérez, Irene Jiménez-Guerrero, Ana Sánchez-Reina, Cristina Civantos, Natalia Moreno-de Castro, Patricia Bernal* and Francisco Pérez-Montaño*.

Affiliation: Departamento de Microbiología, Facultad de Biología, Universidad de Sevilla, Avda. Reina Mercedes 6, Sevilla, Spain

*Address correspondence to Francisco Pérez-Montaño and Patricia Bernal, fperezm@us.es and pbernal@us.es

All authors have seen and approved the manuscript.

Abstract: For agriculture, the symbiosis between rhizobia and legumes is one of the most important relationships economically and environmentally. In this process, the bacteria colonize the roots of the plants, inducing the formation of an organ called a nodule. Within these structures, rhizobia perform biological nitrogen fixation, thereby reducing the demand for this element critical to plant growth. Different bacterial secretion systems (such as the Type X Secretion System, TXSS) have been implicated in establishing this symbiosis, with the T3SS being the most studied. Interestingly, although the T6SS is widely distributed among rhizobia, its role in symbiosis with legumes remains unknown. This system is commonly used as an antimicrobial weapon, although some bacteria utilize it to manipulate eukaryotic cells. In this work, we characterized the T6SS of *Sinorhizobium fredii* USDA257, a fast-growing bacterium with a broad host range. *S.*

fredii USDA257 possesses a unique cluster of T6SS that not only contains genes encoding all the structural components of the system but also includes two genes encoding potential effectors that could target the cell wall of plant cells. Through regulation and secretion assays, we have demonstrated that the system is active and can be induced in nutrient-poor culture media. Additionally, nodulation assays between *S. fredii* USDA257 and its natural host, *Glycine max* var Pekin, seem to indicate that the T6SS plays a positive role in symbiosis.

Keywords: rhizobium, legume, symbiosis, nodulation, competition, type VI secretion system, effector.

1. Introduction

Soil microorganisms generically known as rhizobia belong mostly to the class α-Proteobacteria. These soil-borne microorganisms are located mainly on root and surrounding area, the rhizosphere, where they find an appropriate environment for development. Rhizosphere provides rhizobia protection against desiccation, temperature, and light stress, and supplies suitable nutrients since roots exude large amounts of amino acids, organic acids, sugars, aromatic compounds and secondary metabolites (Walker et al., 2003). One of these secondary metabolites, the flavonoids, initiates the molecular dialogue between rhizobia and legume that culminates with the formation of a new organ in roots, called nodule, where takes place the bacterial reduction of atmospheric nitrogen to ammonia, that can be assimilated by the plant (Oldroyd & Downie, 2008). Thus, when recognized by appropriate rhizobia, flavonoids generate the production of rhizobial signal molecules called nodulation factors (Nod factors). These signal molecules can be specifically recognized by legume plants that initiate the nodulation process that will culminate with nodule development, its occupation and the transformation of the rhizobium into a nitrogen-fixing cell, the bacteroid (Oldroyd et al., 2011). Besides to the initial molecular recognition mediated by flavonoids and Nod factors, it is crucial for the success during nodulation process the compatibility of other types of bacterial molecules. Among these molecules we found proteins secreted through the type III secretion system (T3SS), whose synthesis is also induced in the presence of inducing flavonoids (F. López-Baena et al., 2016). Another protein secretion system, the type VI secretion system (T6SS), can play in some cases a positive or negative role during the symbiosis. Whereas this system is not involved in the nodulation process but rather is on competitiveness in *Paraburkholderia phymatum* and *Azorhizobium caulinodans* (de Campos et al., 2017; H.-H. Lin et al., 2018), the T6SS of *Rhizobium etli* and *Rhizobium leguminosarum* play

different roles in the interaction with host plants, being positive in case of *R. etli* but negative for *R. leguminosarum* (Bladergroen et al., 2003; Nelson & Sadowsky, 2015; Salinero-Lanzarote et al., 2019). In case of *R. etli*, although the inducing molecules have not been yet identified, it was described that this T6SS is synthetized at high cell densities, in the presence of root exudates and within host-plant nodules.

Curiously, this protein secretion system was described for the first time in *Rhizobium leguminosarum*, although the term was not stablished until 2006 when the T6SS of *Vibrio cholerae* and *Pseudomonas aeruginosa* were identified and characterized simultaneously (Mougous, 2006; Pukatzki et al., 2009). T6SS is present in 25% of Gram-negative bacteria, mainly in the Proteobacteria phylum, where the α-, β- and γ-proteobacteria classes are included. This secretion system secretes effectors/toxins essentially into prokaryotic cells, playing an essential role in the competition between bacteria for the same ecological space. However, some effectors target eukaryotic cells and, in this case, T6SS is involved in the success during the infective process (Boyer et al., 2009).

T6SS is a multiprotein complex composed by thirteen main constituents. Genes encoding for these proteins are grouped in the same gene cluster and are called *tss* (type six secretion). Additionally, there is a set of genes that encode for accessory proteins with complementary functions named *tag* genes (type six accessory genes). These genes are not found in all T6SS and carry out different functions such as control of the system assembly and its regulation. T6SS is structured in three main parts: membrane complex (TssJ, TssL and TssM), base plate (TssA, TssK, TssE, TssF and TssG) and tail (TssA, TssB, TssC, Hcp, VrgG and PAAR) (Silverman et al., 2012). Connected to or located inside of this needle-shape structure are found the effectors, that are released into the intracellular environment by sheath contraction (TssA, TssB and TssC proteins). The sheath, which remains in the cytosol, is then disassembled by means of an AAA+ATPase,

known as ClpV (also named TssH), which plays a crucial role in the system recycling (Cherrak et al., 2018) (**Figure 2**).

Genes encoding effector/toxin proteins, which are molecules secreted through the same T6SS and usually inhibit the growth of the target cell, can be often found inside the T6SS cluster. These genes are usually located downstream of the genes encoding the VgrG, Hcp and PAAR proteins. In some cases, effectors are encoded in the same gene that encodes the Hcp, VgrG or PAAR proteins and, therefore, are fused to them in the C-terminal end (**Figure 3**). In this case, the structural proteins are termed evolved proteins (Hcp_e, $VgrG_e$ or $PAAR_e$) (Durand et al., 2014). Effectors can target both eukaryotic and prokaryotic cells, behaving in this last case like toxins. Thus, among the antibacterial toxins we find amidases, peptidoglycan hydrolases, phospholipases and nucleases, which are directed towards the periplasm, the membrane or the cytoplasm of the competitor bacteria. For this reason, it is essential that bacteria possessing a functional T6SS also produce immune proteins for inactivating these toxins, avoiding being their target. In case of those that target eukaryotic cells, effectors are involved in host manipulation processes in order to promote bacterial infection.

Sinorhizobium fredii USDA257 (hereafter USDA257), which presents both T3SS system and T6SS, is one of the best characterized rhizobia so far. This fast-growing rhizobium was isolated from wild soybean but is also able to nodulate a wide variety of legume genera (Pueppke & Broughton, 1999). Thus, USDA257 is one of the most versatile rhizobia along with other rhizobia of the same species, *S. fredii* NGR234 and *S. fredii* HH103, which also have T3SS but not T6SS. The T3SS of USDA257 has been extensively studied and plays a prominent role in symbiosis and in the determination of rhizobial host-range (Staehelin & Krishnan, 2015), since recognition by legume of some type 3 effectors can exert positive (induction of nodulation) or negative (inhibition of

nodulation) roles depending on the cultivar. However, ecological and physiological function of the USDA257 T6SS is completely unknown.

In this work, we performed an exhaustive *in silico* analysis of the T6SS cluster of USDA257, identifying genes involved in the synthesis of all components of the T6SS and several potential effectors. Despite no antimicrobial activity derived from this protein secretion system was observed in competition assays, we found that expression of T6SS is specially enhanced at stationary phase in YM3 minimal medium. Interestingly, the presence of genistein, a *nod* gene inducing-flavonoid, increased the transcriptional activation levels of some genes of the *tss* cluster, pointing to a putative role of this protein secretion system in symbiosis. This hypothesis was confirmed in nodulation tests, assigning a positive role to the USDA257 T6SS during the nodulation process with *Glycine max* cv Pekin, its natural host.

2. Materials and Methods

2.1. Bioinformatical analysis

Sequences of 161 TssB proteins from 153 strains belonging to 12 genera were obtained and compiled by using the BLASTp tool from NCBI website (Boratyn et al., 2013). Sequences were aligned with the ClustalW software (Sievers et al., 2011) and the construction of the phylogenetic tree was carried out using the MEGA7 software (Kumar et al., 2016) applying the Maximum Likehood algorithm (Le et al., 2008) and a JTT matrix model (bootstrap value=500). The phylogenetic tree was customized with the iTOL tool (Letunic & Bork, 2016).

BLASTp analyses were performed at the NCBI website (Boratyn et al., 2013) and amino acid sequence searches using SMART (Letunic et al., 2015) and Pfam (Finn et al., 2016). The Protein Homology/analogy Recognition Engine (Phyre2) server was used to

perform structural-base homology prediction (Kelley et al., 2015). Molecular weight and isoelectric point for each protein were calculated with the ExPaSy software (Artimo et al., 2012). PSORTb server was used to predict sub-cellular location of proteins (Yu et al., 2010), TMHMM software to predict transmembrane domains (Krogh et al., 2001), and SignalP and PSORTb to predict signal peptides (Almagro Armenteros et al., 2019). The figures for the cluster alignments were created using Easyfig (Sullivan et al., 2011).

2.2. Bacterial strains and plasmids

Bacterial strains and plasmids used in this work are listed in Table 1. Rhizobial strains used in this study were grown at 28 °C on tryptone yeast (TY) medium (Beringer J. E., 1974) or yeast extract mannitol (YM) medium (Vincent, 1970) (Bertani, 1951)with two different mannitol concentrations (3 or 10 g mL^{-1}, YM3 or YM10, respectively). *Escherichia coli* strains were cultured on LB medium (Bertani, 1951) at 37 °C. When required, the media were supplemented with the appropriate antibiotics as previously described (Lamrabet et al., 1999). Genistein was dissolved in ethanol and used at 1 µg ml^{-1} to give a final concentration of 3.7 µM.

Table 1. Bacterial strains and plasmid used in this study.

Strain or plasmid	Relevant properties	Source or reference
Sinorhizobium fredii		
USDA257	Wild-type strain, Rif^R	(Pueppke & Broughton, 1999)
USDA257 *tssA*	USDA257 *tssA*::pK18mob, Rif^R Km^R	This work
USDA257 (pMP92::*hcp*-HA)	Wild-type strain with the *hcp*-HA fusion harbored in pMP92 plasmid; Rif^R, Tc^R	This work
USDA257 *tssA* (pMP92::*hcp*-HA)	*tssA* strain with the *hcp*-HA fusion harbored in pMP92 plasmid; Rif^R, Tc^R	This work
USDA257 (pMP220::P_{tssA})	Wild-type strain carrying plasmid pMP220::P_{tssA}; Rif^R, Tc^R	This work

USDA257 (pMP220::P_{ppkA})	Wild-type strain carrying plasmid pMP220::P_{ppkA}; Rif^R, Tc^R	This work
USDA257 (pMP240)	Wild-type strain carrying plasmid pMP240; Rif^R, Tc^R	This work
Agrobacterium tumefaciens		
C58 (pRL662::*gfp2*)	Wild-type strain carrying the GFP fluorescent marker, Gm^R	(Bernal et al., 2017)
Pectobacterium carotovorum		
SCRI 194 (pRL662::*gfp2*)	Wild-type strain carrying the GFP fluorescent marker, Gm^R	(Bernal et al., 2017)
Escherichia coli		
DH5α	*supE44 ΔlacU169 hsdR17 racA1 endA1 gyr96 thi-1 relA1*	Stratagene (USA)
DH5α (pRL662::*gfp2*)	*E. coli* DH5α carrying the GFP fluorescent marker, Gm^R	(Bernal et al., 2017)
Plasmids		
pRK2013	Helper plasmid, Km^R	(Figurski & Helinski, 1979)
pRL662::*gfp2*	Plasmid expressing the GFP2, Gm^R	(Bernal et al., 2017)
pK18mob	Cloning vector, suicide in rhizobia, Km^R	(Schäfer et al., 1994)
pMP220	Cloning vector, empty plasmid, Tc^R	(Spaink et al., 1987)
pMUS1480	pK18mob plasmid carrying an internal fragment of the USDA257 *tssA* gene, Km^R	This work
pMP220::P_{tssA}	pMP220 plasmid carrying the transcriptional fusion between the USDA257 *hcp* promoter region and the *lacZ* gene, Tc^R	This work
pMP220::P_{ppkA}	pMP220 plasmid carrying the transcriptional fusion between the USDA257 *tssA* promoter region and the *lacZ* gene, Tc^R	This work
pMP240	pMP220 plasmid carrying the transcriptional fusion between the *R. leguminosarum* bv. *viciae nodA* promoter and the *lacZ* gene, Tc^R	(de Maagd et al., 1988)
pMP92::*hcp*-HA	pMP92 plasmid carrying the transcriptional fusion between *hcp* and the HA epitope, Tc^R	This work

Plasmids were transferred from *E. coli* to *Sinorhizobium* strains by triparental conjugation as described by Simon using plasmid pRK2013 as helper (Figurski & Helinski, 1979; Simon, 1984). Recombinant DNA techniques were performed according

to the general protocols of Sambrook et al. (Sambrook et al., 1989). PCR amplifications were performed as previously described(F. J. López-Baena et al., 2009). Primer pairs used for the amplification of the *S. fredii* USDA257 genes are summarized in Table 2.

Table 2. DNA oligonucleotide primers used in this study.

Name	**Sequence**	**Usage**
tssA_ecoRI-F	5'- ATAGAATTCATGGGCGATTCCACGAAC	Amplification of an internal fragment of *tssA* gene
tssA_bamHI-R	5'- ATAGGATCCGTCGCCCAATAACCCATC	
Phcp-F	5'- AAAGAATTCCGATATTGCCGCCTTCATC	Amplification of the *hcp* gene and its promoter region.
hcpHA-R	5'- AAAGGATCCTCAAGCGTAATCTGGAACATCG TATGGGTACTTGCCGACATAGACATCCA	
PtssA_ecoRI-F	5'- ATATGAATTCACGGCGACAAGTCCGAAC	Amplification of the promoter region of *ttsA* gene
PtssA_xbaI-R	5'- ATAATCTAGATCGAACAACAGATCCCCCC	
PppkA-F	5'- ATATGAATTCACCTCTTCGGATCCGAACTG	Amplification of the promoter region of *ppkA* gene
PppkA-F	5'- ATAATCTAGAGTAGGTGTTGTTGAGCACCT	
qhcp-F	5'- AAGACCAAGCTGTCGCTC	*q*PCR assays
qhcp-R	5'- ATGTCGAAGCTGTCGCTG	
qppkA-F	5'- ATACGCTGATCGTCATCC	*q*PCR assays
qppkA-F	5'- GCCTTCCTTGACCATGAG	
qtssA-F	5'- TGCTGAATTCCTCGGAAG	*q*PCR assays
qtssA-R	5'- CAGCATCGACTTGACGAA	
q16S-F	5'- TAAACCACATGCTCCACC	*q*PCR assays
q16S-R	5'- GATACCCTGGTAGTCCAC	

An internal fragment of the USDA257 *tssA* gene was amplified using specific primers and the resulting DNA fragment was digested with *Eco*RI and *Bam*HI (both restriction sites were added in forward and reverse 5´ primer ends, respectively) and cloned into pK18mob that was previously digested with same enzymes obtaining plasmid pMUS1480. These plasmids were employed for the homogenotization of the mutated version of the *tssA* gene in *S. fredii* USDA257 generating the mutant strain. Double

recombination events were confirmed by southern blot and PCR (data not shown). For hybridization, DNA was blotted to Hybond-N nylon membranes (Amersham, UK), and the DigDNA method of Roche (Switzerland) was employed according to the manufacturer's instructions. Promoter of two different USDA257 T6SS genes (*tssA* and *ppkA*) were amplified with specific primers (566 and 575 bp, respectively) and the resulting DNA fragment was digested with *Eco*RI and *Xba*I (both restriction sites were added in forward and reverse 5´ primer ends, respectively) and cloned into plasmid pMP220 upstream of the *lacZ* gene that was previously digested with same enzymes, obtaining plasmids pMP220::P_{tssA} and pMP220::P_{ppkA}. Finally, the *hcp* gene and its promoter region were amplified with specific primers (936 pb) adding at the end of the ORF the nucleotides coding for the HA epitope. The resulting DNA fragment was digested with *Eco*RI and *Bam*HI (both restriction sites were added in forward and reverse 5´ primer ends, respectively) and cloned into plasmid pMP92 that was previously digested with same enzymes, obtaining plasmids pMP92::*hcp*-HA. All plasmids were transferred from *E. coli* to USDA257 and/or its *ttsA* derivative by conjugation as previously described using plasmid pRK2013 as helper (Simon, 1984). Recombinant DNA techniques were performed according to the general protocols of Sambrook *et al.* (Sambrook et al., 1989). PCR amplifications were performed as previously described (Jiménez-Guerrero et al., 2015). Plasmids and primers used in this study are listed in **Table 1 and 2**, respectively.

2.3. Determination of β-galactosidase activity.

To determinate the β-galactosidase activity, the wild-type strain was conjugated with the plasmids pMP220::P_{tssA}, pMP220::P_{ppkA} and pMP240, that contains transcriptional fusions between the *tssA* (USDA257), *ppkA* (USDA257) and *nodA* (*R. leguminosarum*) promoters, respectively, and the *lacZ* gene. Assays of β-galactosidase activity were

carried out as described by Zaat *et al* (Zaat et al., 1987). Units of β-galactosidase activity were calculated according to Miller (Miller, 1972). The experiments were repeated at four times with three technical replicates each time.

2.4. RNA extraction and qRT-PCR experiments

Total RNA was isolated using a High Pure RNA Isolation Kit (Roche, Switzerland), according to the manufacturer's instructions. Verification of the amount and quality of total RNA samples was carried out using a Nanodrop 1000 spectrophotometer (Thermo Scientific, USA) and a Qubit 2.0 Fluorometer (Invitrogen, USA). Two independent total RNA extractions were obtained for each condition. This (DNA-free) RNA was reverse transcribed into cDNA by using PrimeScript RT reagent Kit with gDNA Eraser (Takara, Japan). Quantitative PCR was performed using a LightCycler 480 (Roche, Switzerland) with the following conditions: 95 °C, 10 min; 95 °C, 30 s; 50 °C, 30 s; 72 °C, 20 s; forty cycles, followed by the melting curve profile from 60 to 95 °C to verify the specificity of the reaction. The *S. fredii* USDA257 16S rRNA gene was used as an internal control to normalize gene expression. The fold-changes of four biological samples with three technical replicates of each condition were obtained using the ΔΔCt method (Pfaffl, 2001). Selected genes and primers are listed in **Table 2**.

2.5. Purification and analysis of extracellular proteins

Extracellular and intracellular proteins were recovered from 50 ml of YM3 rhizobial cultures grown on an orbital shaker (180 rpm) for 40 h (stationary phase, approximately 10^9 bacteria ml^{-1}). Cultures were centrifuged for 20 min at 10000 g at 4 ºC. Bacterial pellets were normalized and added directly to 300 µl of sample buffer (62.5 mM Tris-HCl [pH 6.8], 2% SDS [m/v], 10% glycerol [v/v], 5% β-mercaptoethanol [m/v], and

0.001% bromophenol blue [m/v]), whilst the culture supernatants were collected and precipitated with trichloroacetic (TCA) acid overnight at -20 ºC. The mixtures were centrifuged for 45 min at 22000 g at 4 ºC. Dried pellets were resuspended in 300 µl of sample buffer. For immunostaining, extracellular proteins were separated on SDS 15% (m/v) polyacrylamide gels and electroblotted to Immun-Blot polyvinylidene difluoride membranes (Bio-Rad, USA) using a Mini Trans-Blot electrophoretic transfer cell (Bio-Rad). Membranes were blocked with TBS containing 2% (m/v) bovine serum albumin (BSA) and then incubated with antibodies raised against the HA epitope (Cell Signaling Technology, USA) diluted 1:1000 in the same solution. Anti-rabbit immunoglobulin AP-conjugated secondary antibody was used and reaction results were obtained using CDP Start Detection Reagent kits (GE Healthcare, USA) according to manufacturer's instructions. Bands were visualized using an ImageQuant LAS 500 imaging workstation instrument (GE Healthcare, USA).

2.6. Interbacterial competition assays

In vitro competition assays were performed on YM3 (prey) agar (2% w/v) plates, as previously described (Bernal et al., 2021). Briefly, overnight bacterial cultures were washed and adjusted to an OD_{600} of 1.0 in sterile PBS, and mixed at a 1:1 ratio (USDA257:prey). Mixtures were grown on YM3 agar plates at 30 °C for 24 or 48 hours and then collected using an inoculating loop and resuspended in sterile PBS. The outcome of the competition was quantified by counting colony forming units (CFUs) using antibiotic selection of the input (time = 0 hours) and output (time = 24-48 hours). All prey strains harbored the plasmid pRL662, which confers resistance to gentamicin and was used for antibiotic selection, whereas *S. fredii* USDA257 is naturally resistant to rifampicin. Competition assays were performed at least three biologically independent

experiments. Competitive index values were calculated using the following formula: competitive index = (output attacker/output prey)/(input attacker/input prey).

2.7. Nodulation assays

For the evaluation of the symbiotic phenotypes, the wild-type and derivative mutant were grown in YM3 medium. Surface-sterilized seeds of *G. max* cv Pekin were pre-germinated and placed in sterilized Leonard jars and test tubes respectively, containing Fårhaeus N-free solution (Vincent, 1970). Germinated seeds were then inoculated with 1 mL of bacterial culture in a concentration approx. 10^9 cells mL^{-1}. Growth conditions were 16 h at 26 ºC in the light and 8 h and 18 ºC in the dark, with 70% of humidity. Nodulation parameters were evaluated after 6 weeks. Shoots were dried at 70 ºC for 48 h and weighed. Nodulation experiments were performed three times with five replicates for each treatment. For the different parameters analysed, the values of each treatment were compared to those of USDA257 wild-type strain by using the ANOVA test.

3. Results

3.1. Genome-wide screening for T6SSs in Rhizobiales order

In silico analyses revealed the presence of 160 TssB proteins from 13 different genera in *Rhizobiales* order (**Table S1**). In **Figure 1** is shown the phylogenetic distribution of these T6SS clusters according to evolutionary distances for the core component protein TssB. Most T6SS systems (140, 87.5%) clustered in groups 3 (54, 33.75%), including the USDA257 T6SS, or group 5 (86, 53.75%). On the other hand, only two members of the *Rhizobiales* order were found in both group 2 and 4 (1.25% each); whereas group 1 contained 14 T6SS clusters (9.75%). *Bacteroides fragilis* TssB, evolutionarily separated from *Proteobacteria* T6SSs, was used as root of the tree.

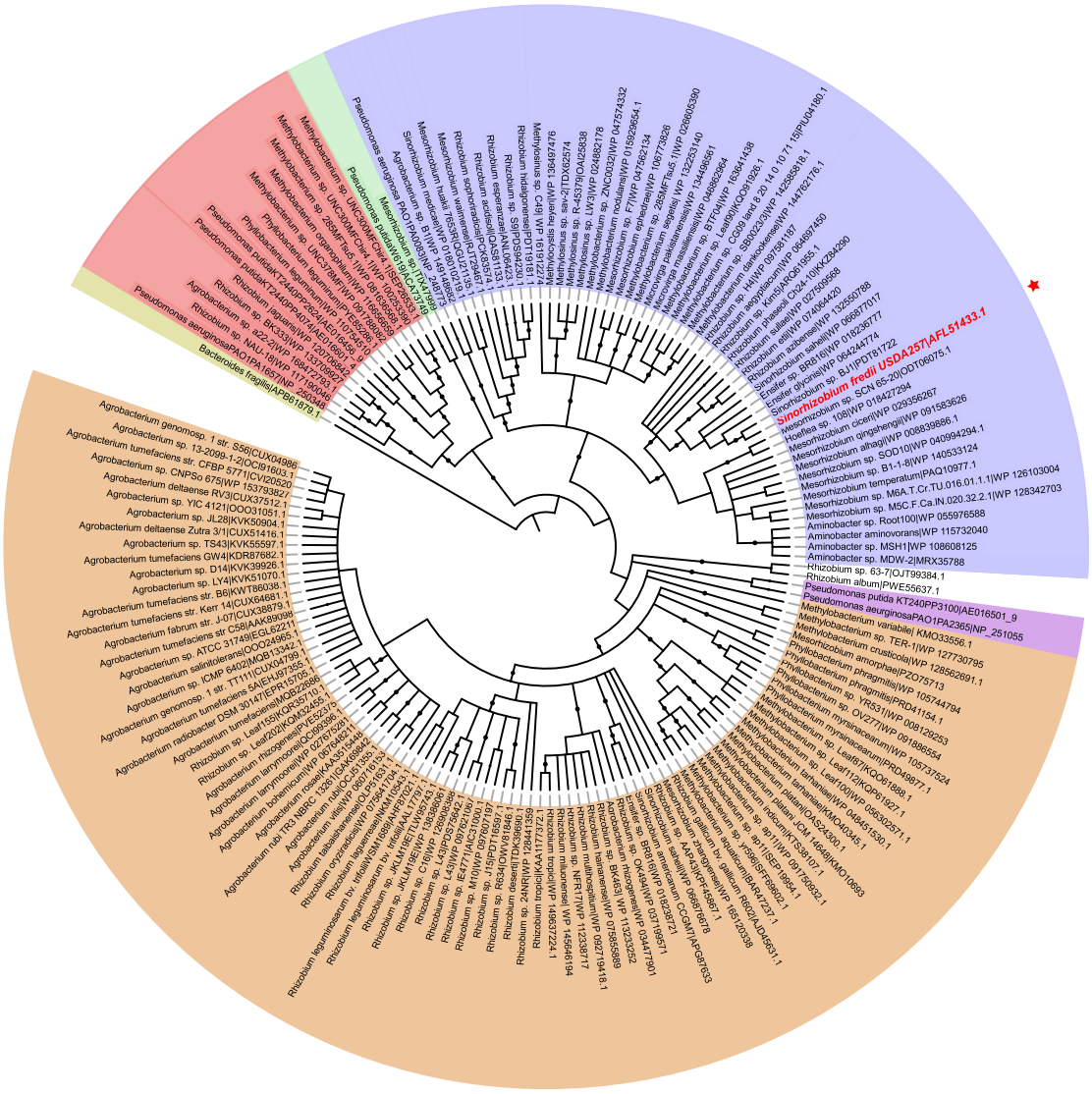

Figure 1. Phylogenetic tree of T6SSs of *Rhizobiales* order. Maximum likelihood tree with 500 bootstrap replicates were built with Mega 7 software for the core component protein TssB. T6SS cluster nomenclature is used to show the main phylogenetic clusters (Boyer et al., 2009). Branches with black circles indicate a confidence level higher than 0.75. Five groups are distinguished: group 1 (red), group 2 (green), group 3 (blue), group 4 (purple) and group 5 (orange). Bacterium of the genus *Bacteroides* (brown) represents the root of the tree. Red star indicates the position of the *S. fredii* USDA257 T6SS.

3.2. The reference rhizobial strain S. fredii USDA257 possesses a complete T6SS

Inspection of the genome of *S. fredii* USDA257 revealed 26 T6SS-related ORFs located in one chromosomal cluster (**Figure 2**). From these, fourteen encode for the all

structural proteins required for a functional T6SS: membrane complex (TssJ, TssM, TssL), TssA, base plate (TssE, TssF, TssG, TssK), contractile sheath (TssB, TssC), inner tube (Hcp), needle (VrgG, PAAR) and ATPase (ClpV). Moreover, we found genes coding for the PpkA, PppA, TagF and Fha regulatory proteins (**Figure 2**).

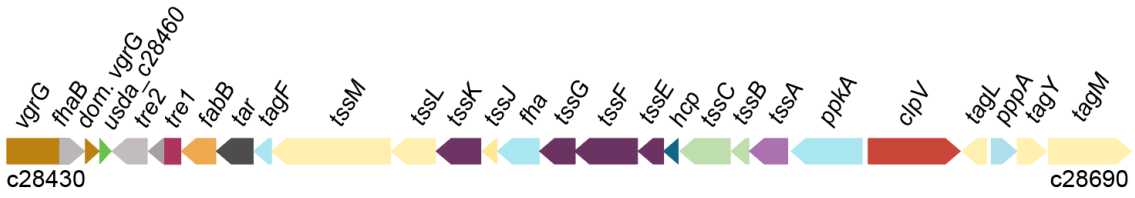

Figure 2. Organization of the T6SS cluster of *S. fredii* USDA257. Color codes: Genes that encode the components of membrane complex (*tssMLJ*) and accessory proteins (*tagLYM*) (veige). Genes coding for components of the base plate (*tssKGFE*) (magenta). *tssA* (violet). Genes *tssB* and *tssC* (contractile sheath) (light green). The *hcp* gene, that encodes the protein forming the inner tube (dark blue). Genes that encode regulatory proteins (*tagF*, *fha*, *ppkA* and *pppA*) (light blue). *clpV*, that codes for ATPase (red). Genes coding for possible effectors of the system (*vgrG*$_e$, *tre2* and *tre1*) (grey). Gene that encodes a possible adapter (*tar*) (dark gray). Gene of unknown function (*usda_c28460*) (green). The *vgrG* genes (brown). *paar* (pink).

An in deep analysis of the T6SS membrane complex components of *S. fredii* USDA257 showed that TssL possesses a DotU domain (between 43-246 aa), which directly binds to the IcmF domains of the TssM protein. Moreover, TssL has a transmembrane domain and, at the C-terminal end (Ct), a peptidoglycan binding domain (OmpA), which define it as a specialized TssL. Prediction of cell localization also indicates that TssL is located on the inner membrane (**Figure 3**). The other protein of membrane complex, TssM, is composed of three transmembrane domains and three conserved DotU-binding domains (IcmF), two of them located in the amino terminal end (Nt). Prediction of cellular localization indicates that TssM is also found in the inner membrane of the bacterium (**Figure 3**). Regarding to accessory proteins of the membrane

complex, USDA257 also possesses TagL. This structural protein shares certain degree of homology with both TssM and TssL proteins, since it contains both a DotU-binding domain and a peptidoglycan-binding domain. TagL also has a periplasmic signal peptide at the Nt end, predicting its location in the bacterial periplasm (**Figure 3, Figure S1**). Interestingly, two Ct DotU-binding domains, a single transmembrane domain, and a Nt DotU domain appear also in a specific protein of this cluster, named as TagM. Despite TagM presents the same localization probability in all subcellular compartments, its transmembrane domain and the absence of specific signal peptides could indicate that this protein is located in the inner membrane (**Figure 3, Figure S1**).

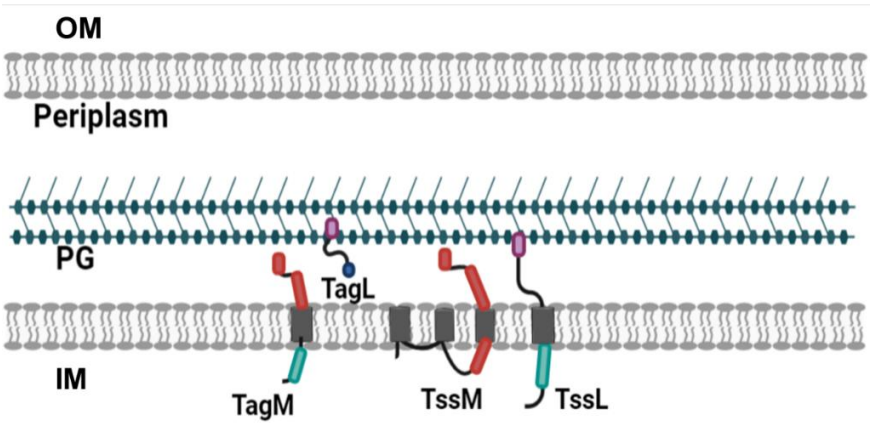

Figure 3. Schematic representation of the structural proteins TssM, TssL, and the accessory TagL and TagM and their corresponding domains. DotU cytosolic domain (green), transmembrane domain (dark gray), IcmF structural domain (red), OmpA peptidoglycan-binding domain (purple), and signal peptide (blue). OM: outer membrane, IM: inner membrane, PG: peptidoglycan layer.

Lastly, between *tagL* and *tagM* genes is located another gene coding for a protein with two domains that we have named *tagY* (**Figure 2**). Nt end belongs to the SlyX superfamily domain (Pfam04102), with unknown function; whilst Ct part clusters in the peptidase M15_4 domain (Pfam13539), corresponding to a D-alanyl D-alanine carboxypeptidase.

Predictions indicate that TagY has a transmembrane domain at the Nt end and a signal peptide, suggesting that this protein could be anchored to the outer membrane, with the Ct end facing the periplasm or to the cellular exterior.

3.3. *The S. fredii USDA257 cluster harbors genes coding potential effectors*

The USDA257 *vrgG* and *PAAR* genes encode for evolved proteins, $VgrG_e$ and $PAAR_e$, in which Ct ends contain putative effector domains (Pukatzki et al., 2009). According to sequence similarity, the Ct domain of $VgrG_e$ corresponds to a 225 amino acid fragment from the FhaB protein, a chaperone that prevents the premature folding of hemagglutinin filaments (FHA), one of the virulence factors of *Bordetella pertussis* (Coutte et al., 2001). Interestingly, taking into consideration the analysis performed with Phyre2 software this Ct domain also shows structural homology with the Cthe_2159 protein from *Hungateiclostridium thermocellum* ATCC 27405 (85% alignment, 86.5% confidence), a polysaccharide lyase-type protein that binds to cellulose and polygalacturonic acid. In contrast, protein encoded by USDA257_c28480 possesses a PAAR domain at the Nt end and an effector domain with unknown function and without any structural homology at the Ct end, named as Tre1 (*tre*, type six rhizobial effector) (**Figure 2, Table 3**).

Rest of genes coding effectors / toxins of the T6SS are usually located downstream of the $vgrG_e$ and, if present, T6SS adapter genes. In *S. fredii* USDA257 structure of this region is inverted since USDA257_c28500 (*tar*, type six adapter rhizobium), USDA257_c28480 ($PAAR_e$ or *tre1*) and USDA257_c28470 (*tre2*) genes are orientated oppositely than $vgrG_e$ (USDA257_c28430). The *tar* product possesses a DUF2169 superfamily domain that has been identified in previous studies as a T6SS adapter (**Figure 2, Table 3**) (Lien & Lai, 2017; Pissaridou et al., 2018). Thus, protein encoded by the USDA257_c28470 gene was named Tre2 due to its possible role as an effector.

According to Phyre[2], Tre2 shows structural homology with a glycoside hydrolase enzyme (GH74) with a xyloglucan binding domain from *Caldicellulosiruptor lactoaceticus* 6A (69% alignment, 99.3% confident) (**Figure 2, Table 3**).

Table 3. Genes of the T6SS cluster of *S. fredii* USDA257.

Locus name	Protein name	Conserved domains[a]	Celullar localization prediction
USDA257_c28440	$VgrG_e$	COG3501 (VgrG) + COG3210 (FhaB)/ pfam06715 (Gp5_C)	C
USDA257_c28450	VgrG dom	COG3501 (VgrG)/ TIGR01646 (Vrg_GE)	D
USDA257_c28460		TIGR02270	C
USDA257_c28470	Tre2	Glycosyl hydrolase GH74	C
USDA257_c28480	Tre1	PAAR-pfam13665 (DUF4150)	C
USDA257_c28490	FabB	COG0304 (FabB)	MI
USDA257_c28500	Tar	DUF2169	C
USDA257_c28510	TagF	COG3913 (SciT)	D
USDA257_c28520	TssM	COG3523 (IcmF)	MI
USDA257_c28530	TssL	COG3455 (DotU) + Pfam00691 (OmpA)	ME
USDA257_c28540	TssK	COG3522	C
USDA257_c28550	TssJ	COG3521	MI
USDA257_c28560	Fha	COG3456	C

USDA257_c28570	TssG	COG3520	C
USDA257_c28580	TssF	COG3519	C
USDA257_c28590	TssE	COG3518	C
USDA257_c28600	Hcp	COG3157 (Hcp)	C
USDA257_c28610	TssC	COG3517	C
USDA257_c28620	TssB	COG3516	C
USDA257_c28630	TssA	COG3515 + TIGR03363	C
USDA257_c28640	PpkA	COG0515 (SPS1)	P + PC
USDA257_c28650	CIpV	COG0542 (CIpA) + pfam07724 (AAA_2)	C
USDA257_c28660	TagL	COG2885 (OmpA)	ME
USDA257_c28670	PppA	COG0631 (PTC) + TIGR02865 (spore_II_E)	C
USDA257_c28680	TagY	Pfam04102 (SlyX) + pfam13539 (peptidasa_M15_4)	D
USDA257_c28690	TagM	COG3523 (IcmF) + COG3455 (DotU)	D

OM: outer membrane, IM: inner membrane, C: cytoplasmic, P: periplasm, PC: cell wall, D: unknown, aa: amino acid.

a: conserved domains according to COG / pfam / TIGR / Phyre[2].

3.4. *The vrg$_e$ cluster is well conserved among rhizobia excepting for the effector region*

To obtain a broader perspective of functioning and distribution of *tre1* and *tre2* genes among rhizobia, we performed a comparison of the *vgrG$_e$* clusters from eighteen rhizobial strains. In **Figure 4** is showed the high conservation of sequence across the entire cluster, with the noticeable exception of the region coding Tre1 and Tre2 domains.

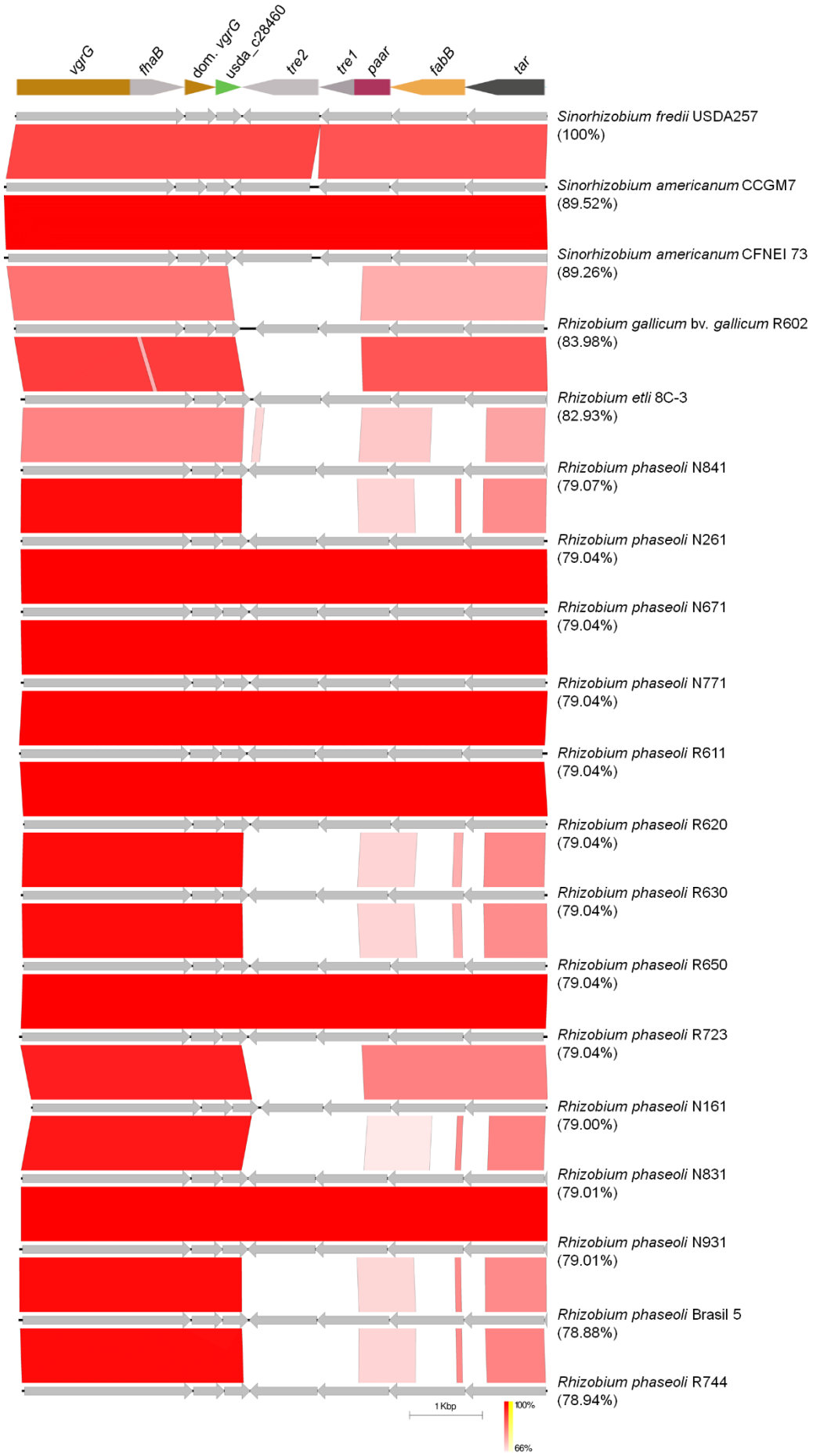
vgrG
fhaB
dom. vgrG
usda_c28460
tre2
tre1
paar
fabB
tar
Sinorhizobium fredii USDA257 (100%)
Sinorhizobium americanum CCGM7 (89.52%)
Sinorhizobium americanum CFNEI 73 (89.26%)
Rhizobium gallicum bv. gallicum R602 (83.98%)
Rhizobium etli 8C-3 (82.93%)
Rhizobium phaseoli N841 (79.07%)
Rhizobium phaseoli N261 (79.04%)
Rhizobium phaseoli N671 (79.04%)
Rhizobium phaseoli N771 (79.04%)
Rhizobium phaseoli R611 (79.04%)
Rhizobium phaseoli R620 (79.04%)
Rhizobium phaseoli R630 (79.04%)
Rhizobium phaseoli R650 (79.04%)
Rhizobium phaseoli R723 (79.04%)
Rhizobium phaseoli N161 (79.00%)
Rhizobium phaseoli N831 (79.01%)
Rhizobium phaseoli N931 (79.01%)
Rhizobium phaseoli Brasil 5 (78.88%)
Rhizobium phaseoli R744 (78.94%)
1 Kbp
100%
66%

367

Figure 4. Genome sequence alignment of the *vgrG$_e$* region demonstrating the divergence of *tre1* and *tre2* in eighteen rhizobial strains using Easyfig. Cluster are sorted by homology degree respect to the VrgG$_e$ protein from *S. fredii* USDA257 (Blastp E value). In parenthesis is indicated the percentage of identity for each VrgG$_e$.

A neighbor-joining phylogeny of the Tre1 and Tre2 proteins from these rhizobial strains clearly grouped both *S. fredii* USDA257 versions with those present in *Sinorhizobium americanum* strains CCGM7 and CFNEI 73, whereas most Tre1 and Tre2 *Rhizobium phaseoli* versions were distributed in two separated branches, one grouping versions from strains R620, R650, R611, N771, N671, N261, R723 and Brasil 5, and the other one clustering proteins from strains N841, R630, N831, N931 and R744 (**Figure 5**).

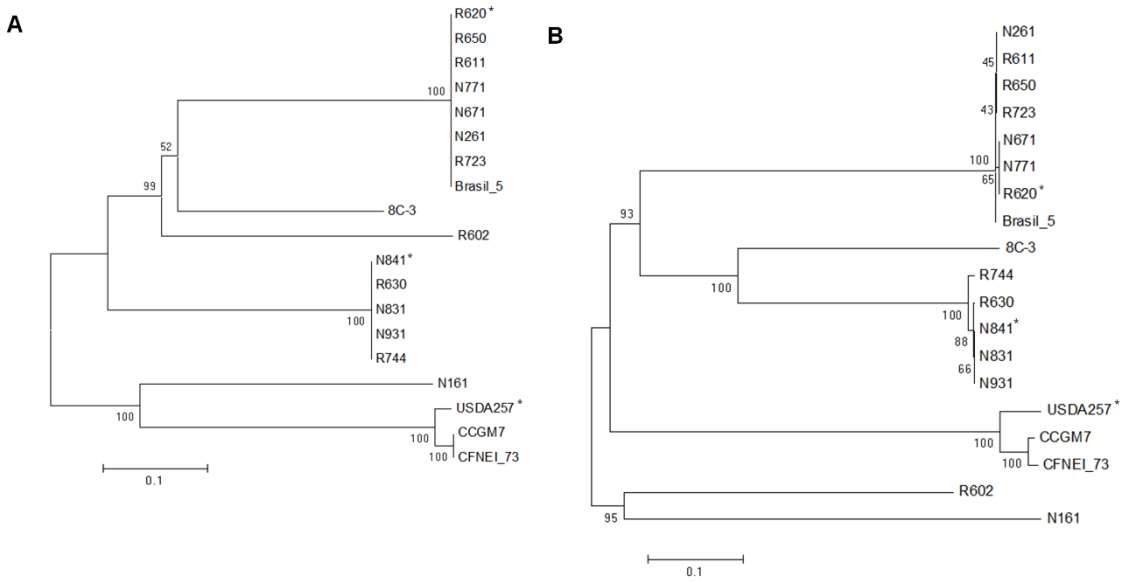

Figure 5. Neighbor-joining tree of several rhizobial strains. Bootstrap values ≥40 are indicated for each node. The cluster analysis to group the strains by Tre1 (A) or Tre2 (B) sequence similarities was done using the program CLUSTALW in the MEGA7 software package with the algorithm neighbor-joining method. Tree robustness was assessed by bootstrap resampling (1000 replicates each). Asterisks indicate representative Tre1 and Tre2 versions for each main branch.

Alignment of the Tre1 protein sequences indicated a high degree of similarity among the N-terminal but not in the C-terminal domains in all versions, that were grouped as in the phylogenetic tree (**Figures S2-4**). As expected, first half of the different versions of Tre1 proteins showed a clear structural homology with PAAR domain (**Table 4**). Interestingly, despite alignment of Tre2 versions showed a lower degree of similarity among proteins from different branches of the phylogenetic tree (**Figures S5-7**), the structural homology predicted by Phyre[2] indicate that these proteins were structurally similar than the same GH74 glycoside hydrolase enzyme, differencing in their range of alignment (**Table 4**).

Table 4. Protein structural homologies from representative versions coded by same loci than *tre1* and *tre2* genes of *S. fredii* USDA257.

Rhizobial strain	Tre1-like	Tre2-like
Sinorhizobium fredii USDA257	PAAR (25-125 a.a., C: 97.4%). Size: 324 a.a.	Glycosyl hydrolase GH74 (1-340 a.a., C: 99.5%). Size: 351 a.a.
Rhizobium phaseoli N841	PAAR (26-126 a.a., C: 97.2%). Size: 328 a.a.	Glycosyl hydrolase GH74 (106-301 a.a., C: 99.1%). Size: 309 a.a.
R. phaseoli R620	PAAR (26-126 a.a., C: 97.3%). Size: 330 a.a.	Glycosyl hydrolase GH74 (98-302 a.a., C: 99.3%). Size: 309 a.a.

Structural homologies were determined by Phyre[2] software. In parenthesis are indicated range of aligned amino acids and confidence of the prediction (C).

3.4. The T6SS of S. fredii USDA257 is induced in YM3 minimal medium

In order to determine the growth conditions in which the T6SS of *S. fredii* USDA257 is expressed, two different but complementary approaches (qRT-PCR and ß-galactosidase assays) were implemented, both measuring the expression levels of the *ppkA* and *tssA* T6SS genes. qRT-PCR experiments of USDA257 bacterial cultures grown at exponential and stationary phases in three different culture media (TY, YM10 and YM3) shed same transcriptional activation trend for both *ppkA* and *tssA* genes, i.e. highest transcriptional values at stationary phases specially in the YM3 minimum medium (11-fold and 7-fold, respectively, in comparison to that values obtained at exponential phase in TY medium) (**Figure 6A**). This activation pattern was similar to that obtained in ß-galactosidase assays by using plasmid constructions containing the *ppkA* and *tssA* promoter regions of USDA257 fused to the *lacZ* reporter gene, that were transferred by conjugation to the wild-type strain. Enzymatic activity levels showed by these strains reinforced YM3 as the most T6SS inducing medium, since for both promoters reached higher increases in the fold-change values when bacteria were grown in this minimum medium (4-fold and 2,5-fold, respectively, in comparison to those values obtained by the strain carrying the empty plasmid) (**Figure 6B**). However, in ß-galactosidase assays activation patterns were in general higher at exponential phases, pointing out a partial saturation or inhibition of the enzymatic reaction when the number of cells is elevated.

To gain insight about the potential role of the T6SS of *S. fredii* USDA257 in the early steps of the symbiotic process, β-galactosidase assays were performed in the presence of genistein, a *nod*-gene inducing flavonoid in several related *S. fredii* strains (Jiménez-Guerrero et al., 2018; Pérez-Montaño et al., 2016; Pérez-Montaño, Jiménez-Guerrero, et al., 2014). Activation of the *ppkA* and *tssA* promoters were measured in YM3 medium in both exponential and stationary phases in the presence or the absence of genistein, using as control of *nod*-gene induction the wild-type strain carrying the pMP240 plasmid, which

harbors the conserved *nodA* promoter of *R. leguminosarum* bv. *viciae* fused to the *lacZ* reporter gene. Interestingly, in the presence of genistein in cultures grown until exponential phases, values of β-galactosidase activity slightly increased in strains carrying the *ppkA* and *tssA* promotors fused to *lacZ*, suggesting that not only the nodulation but also the T6SS genes could be overexpressed in the presence of this flavonoid (**Figure 6C**). Despite these results support a functional T6SS in *S. fredii* USDA257, the secretion of the Hcp protein into a culture medium is considered as the 'hallmark' of a functional T6SS (Pukatzki et al., 2009; Salinero-Lanzarote et al., 2019). To determine whether the T6SS of USDA257 strain is activated in YM3 medium at stationary phase, immunoblots containing protein extracts from supernatant and whole cells containing an Hcp-HA fusion were analyzed using a rabbit anti-HA antiserum. A unique clear band of approximately 17 kDa, the expected mass for Hcp, was detected in the supernatants where the wild-type strain was grown but not in those where the *tssA* strain was inoculated, indicating that this protein secretion systems is fully functional under these conditions (**Figure 6D**).

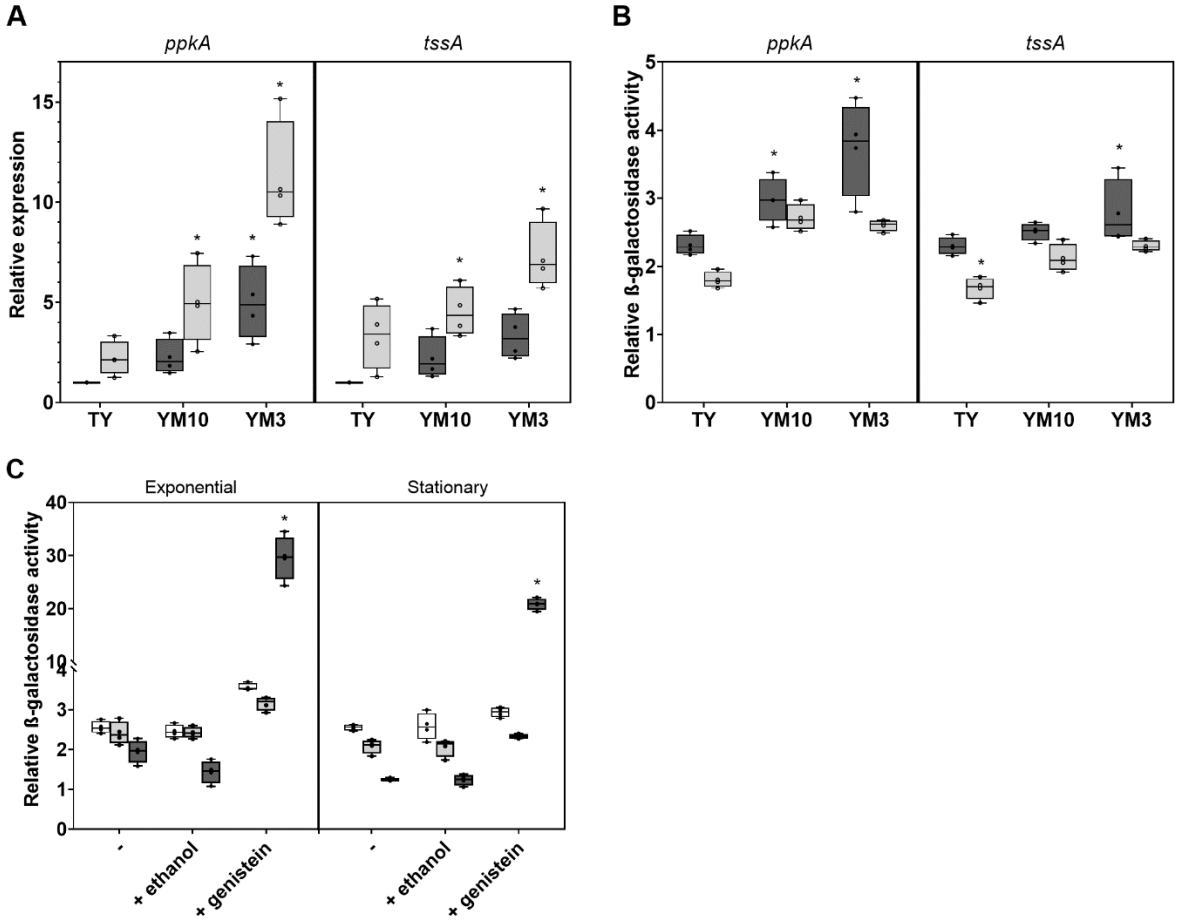

Figure 6. Functionality of the *S. fredii* USDA257 T6SS. (A) Quantitative RT-PCR analysis of the expression of the *ppkA* and *tssA* genes of USDA257 grown in the TY, YM10 and YM3 media until stationary (dark gray boxes) or exponential (light grey boxes) phases. Expression data shown are the mean (± standard deviation of the mean) for four biological replicates. For each gene, expression was calculated relative to the lowest expression detected (TY medium at exponential phase) by using the Two-ways Anova test with multiple comparisons. The asterisks indicate a significant difference at the level α = 5%. (B) Fold-change values of the β-galactosidase activities of USDA257 carrying a plasmid pMP220 which contains the *ppkA* and *tssA* promoters fused to the *lacZ* gene. Assayed conditions were TY, YM10 and YM3 media in both exponential (light grey boxes) and stationary phases (dark grey boxes). Parameters were individually compared with those obtained by each strain in TY medium at exponential phase by using the Two-ways Anova test with multiple comparisons. Values tagged by asterisks (*) are significantly different at the level of α = 5%. (C) Fold-change values of the β-galactosidase activities of USDA257 carrying plasmid pMP220, which contains the *ppkA* (white bars) and *tssA* (light grey bars) promoters fused to the *lacZ* gene, or plasmid pMP240, which contains the conserved *nodA* promoter from *R. leguminosarum* fused to *lacZ* (dark grey bars). Assayed conditions were YM3 medium in both exponential and stationary phases in the absence and in the presence of ethanol or flavonoid. Parameters were individually compared with those obtained by in the wild-type strain carrying the empty vector in YM3 medium by using the Two-ways Anova test with multiple comparisons. Values tagged by asterisks (*) are significantly different at the level of α = 5%. (D) Immunodetection of the HA epitope fused to Hcp in intracellular and

extracellular proteins from cultures of the wild-type and *tssA* mutant strains of USDA257 grown a in YM media at stationary phase.

3.5. The T6SS of S. fredii USDA257 is not involved in interbacterial competition

To gain insight into the role and functioning of the *S. fredii* USDA257 T6SS, we carried out interbacterial competition assays between the wild-type and *ttsA* (T6SS-defective) strains of USDA 257 as predators and the other bacterial species (*E. coli*, *A. tumefaciens* and *P. carotovorum*) as preys. The bacteria were mixed 1:1 (predator:prey) and co-cultured on YM3 inducing medium for 24 hours. Spots containing the competing bacteria were collected and the bacterial CFUs were determined on selective plates. The competitive index of predator bacteria at 24 hours is shown in **Figure 7**. In all cases, these statistically similar values were obtained for both wild-type and *tssA* strains. These competitive index values were between 0 and 1, which indicates that the USDA257 T6SS is not involved in interbacterial competition neither against *E. coli* nor against another potential rhizospheric competitor as the pathogenic *A. tumefaciens* and *P. carotovorum* (Bernal et al., 2017).

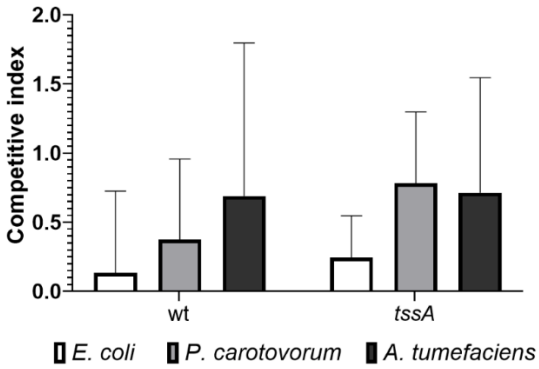

Figure 7. Bactericidal activity of *S. fredii* USDA257 against several species. *E. coli*, *A. tumefaciens* and *P. carotovorum* harbor the pRL662::*gfp2* plasmid that confers gentamycin resistance. The wild type and *tssA* mutant strains were co-incubated with each bacterium for 24 h. Competition assays between USDA257 strains, *E. coli*, and a set of plant rhizobacteria show similar and low competitive index for the mutant compared to the wild-type strain. Statistical analysis was performed using the Two-ways Anova test with multiple comparisons. Values tagged by asterisks (*) are significantly different at the level of $\alpha = 5\%$.

3.6. The T6SS of S. fredii USDA257 is required for a successful symbiosis with G. max cv Pekin

To gain insight into the role and functioning of the *S. fredii* USDA257 T6SS, the symbiotic interactions among the wild-type or *tssA* strains with *G. max* cv Pekin, considered its natural host, were analysed (**Figure 8**). The number of nodules in examined plants inoculated by the *tssA* mutant was statistically lower to those obtained in plants infected by the parental strain. Similar but not statistically trends were observed for both nodule fresh mass and plant-top dry mass parameters. Thus, results obtained from nodulation assays indicate that the T6SS of USDA257 is required for an optimal nodule formation in soybean cv Pekin.

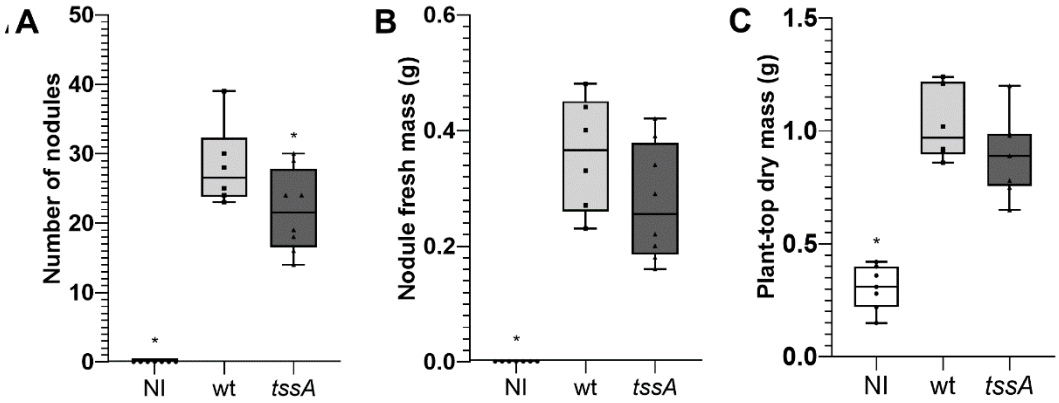

Figure 8. Plant responses to inoculation of *G. max* cv Pekin with different *S. fredii* USDA257 strains. Plants were evaluated 6 weeks. Parameters (A, number of nodules; B, nodule fresh mass; C, Plant-top dry mass) were individually compared with that obtained with the wild-type strain CIAT 899 by using the Two-ways Anova test with multiple comparisons. Values tagged by asterisk (*) are significantly different (α = 5%). NI: non-inoculated plants.

4. Discussion

Application of symbiotic rhizobia is a cheap and ecofriendly alternative source of nitrogen for plants, which favors a moderate use of nitrogen fertilizers mitigating their

excessive utilization (Martinelli et al., 2020; Pérez-Montaño, Alías-Villegas, et al., 2014). The efficiency of symbiosis depends on various factors such as soil, environment and symbiotic pair. From the rhizobia point of view, several molecules are important in this intimate interaction, highlighting Nod factors, extracellular polysaccharides, and protein secretion systems (F. López-Baena et al., 2016). In case of T3SS, numerous examples have been described to have neutral, positive or negative effects on symbiosis depending on the plant host (Nelson & Sadowsky, 2015). However, studies about the role of rhizobial T6SS on symbiosis are very scarce, despite the first report dealing with T6SS indicated that this protein secretion system impairs nodulation between *R. leguminosarum* and pea (Bladergroen et al., 2003). Conversely, a positive effect of T6SS on symbiosis was recently described in the nodulation process between *Rhizobium etli* and bean (Salinero-Lanzarote et al., 2019). In two additional studies, it was demonstrated a role of T6SS on interbacterial competition but not in symbiosis (de Campos et al., 2017; H.-H. Lin et al., 2018). In the case of the *Sinorhizobium* genera, no studies have been performed so far.

T6SSs distributed among *Proteobacteria* phylum are classified in five phylogenetic groups (Boyer et al., 2009). Reference strains for each phylogenetic group belong to the order *Pseudomonadales*, except for group 5, whose reference strain is *Agrobacterium tumefaciens*. TssB is commonly used to group and classify the different T6SSs among the five phylogenetic groups, since this highly conserved protein conforms the contractile sheath of the T6SS in all microorganisms analyzed so far (Bernal et al., 2017; Cascales & Cambillau, 2012). In case of the USDA257, according to its TssB sequence, the T6SS belongs to the group 3, which is one of the most represented phylogenetic groups among the *Rhizobiales* order. An in deep analysis indicate that the genome of USDA257 contains the fourteen genes coding for all structural proteins required for a functional T6SS in one

chromosomal cluster. Besides to these T6SS core proteins, *in silico* analysis points out that USDA257 synthetizes two accessory proteins of the membrane complex, TagL and TagM. Additionally, most T6SSs described so far are controlled by regulatory proteins (J.-S. Lin et al., 2018; Mougous et al., 2007). A well-studied example is the kinase-phosphatase PpkA-PppA couple, which mediates the system formation through a phosphorylation cascade that ends with the structural components assembly. In the case of the USDA257 cluster, we found not only genes coding for PpkA-PppA regulatory proteins but also those encoding the TagF and Fha proteins, which also interact with the system and regulate its activity at post-transcriptional level (J.-S. Lin et al., 2018; Mougous et al., 2007). Genes coding effector proteins are often found inside of the T6SS cluster, specifically in the *vrg* gene neighborhood (Durand et al., 2014). In USDA257, both *vrgG* and *PAAR* genes encode for evolved proteins. The Ct effector domain (FhaB) of $VrgG_e$ seems to have polysaccharide lyase-type activity, which indicates that this USDA257 effector could bind to cellulose and polygalacturonic acid, being involved in the attachment to vegetal cell wall (Pissaridou et al., 2018) Interestingly, Tre2 also shows structural homology with a glycoside hydrolase enzyme with a xyloglucan binding domain able to hydrolyze the plant cell wall (Arnal et al., 2019), suggesting that Tre2 could be involved in the degradation of this structure. Interestingly, sequence and structural comparison of the Tre2 proteins from several rhizobial strains indicate that, despite the sequence dissimilarity found among the three different versions of effector, in all cases Tre2 proteins show structural homology with the same glycoside hydrolase enzyme, suggesting that this function could be conserved among related rhizobia. Finally, in case of the evolved protein coded by *PAAR* gene, the putative Ct effector domain (Tre1) function remains elusive in all analyzed rhizobia and will require further investigation.

Overall, the exhaustive *in silico* analysis performed in this work points to a functional T6SS of *S. fredii* USDA257, which might be involved on the interaction with the host plant cells. But is indeed this T6SS fully functional and involved in the nodulation process? According to our results, the USDA257 T6SS genes are highly expressed in minimal medium, specially at exponential phase and in the presence of *nod*-gene inducing flavonoids of several related bacteria(Pérez-Montaño et al., 2016; Pérez-Montaño, Jiménez-Guerrero, et al., 2014), which strengthens the involvement of this protein secretion system on the early steps of symbiosis. Findings described for the symbiotic the *R. etli* T6SS are in most extend similar, since this protein secretion system is fully functional in yeast mannitol medium in the presence of bean root exudates, where specific *nod* gene inducing-flavonoids are present(Salinero-Lanzarote et al., 2019). Thus, the expected involvement on the symbiotic process of the USDA257 T6SS was confirmed in nodulation assays, where the absence of this protein secretion system reduces the formation of nodules in soybean. In summary, *in vivo* assays confirm what emerged from *in silico* analysis, i.e. this protein secretion system is fully functional exerting a positive effect of T6SS on the symbiosis stablished between *S. fredii* USDA257 and *G. max* cv Pekin, its natural host. Similarly, the T6SS of *R. etli* Mim1 also has a positive effect in symbiosis(Salinero-Lanzarote et al., 2019). However, in this strain, information about its role on bacterial competition is missing.

In our work, to close this gap, we also performed competition assays against several bacteria under T6SS inducing-conditions, outcoming that this protein secretion system does not provide killing ability to USDA257. This result agrees with the *in silico* analysis of putative effectors, since these proteins do not share homology with any antibacterial toxins or immunity proteins. Thus, the involvement of rhizobial T6SS on interbacterial competition seems to be incompatible for its role on symbiosis and *vicerversa*, since both

abilities have never been described at the same time in the same rhizobial strain (Bladergroen et al., 2003; de Campos et al., 2017; H.-H. Lin et al., 2018; Salinero-Lanzarote et al., 2019).

In conclusion, we show a positive role of T6SS in *S. fredii*–legume symbiosis but not in interbacterial competition. Despite possible functions have been suggested for some T6SS effector genes, future work is needed to elucidate their function and functioning to understand the specific role they play in rhizosphere and symbiosis.

Supplementary Materials: Figure S1: Multiple alignment of the TssM, TssL, TagM and TagL sequences. Figure S2-4: Multiple alignment of the Tre1 sequences. Figure S5-7: Multiple alignment of the Tre2 sequences.

Acknowledgments: This work was funded with project PID2020-118279RA-I00 from the Spanish Ministry of Science and Innovation.

Author Contributions: Conceptualization, F.P-M., P.B., and I.J-G.; Methodology, I.J-G., and P.B.; Validation, A.S-R., C.C., N.M-C., F.O., and I.J-G.; Formal Analysis, F.P-M., and I.J-G.; Investigation, A.S-R., C.C., N.M-C., F.O., and I.J-G.; Writing – Original Draft Preparation, F.P-M.; Writing – Review & Editing, P.B.; Visualization, F.P-M., and P.B.; Project Administration, P. B, and F.P-M.; Funding Acquisition, P. B, and F.P-M.

Conflicts of Interest: The authors declare no conflict of interest.

References

Almagro Armenteros, J. J., Tsirigos, K. D., Sønderby, C. K., Petersen, T. N., Winther, O., Brunak, S., von Heijne, G., & Nielsen, H. (2019). SignalP 5.0 improves signal peptide predictions using deep neural networks. *Nature Biotechnology*, *37*(4). https://doi.org/10.1038/s41587-019-0036-z

Arnal, G., Stogios, P. J., Asohan, J., Attia, M. A., Skarina, T., Viborg, A. H., Henrissat, B., Savchenko, A., & Brumer, H. (2019). Substrate specificity, regiospecificity, and processivity in glycoside hydrolase family 74. *Journal of Biological Chemistry*, *294*(36). https://doi.org/10.1074/jbc.RA119.009861

Artimo, P., Jonnalagedda, M., Arnold, K., Baratin, D., Csardi, G., de Castro, E., Duvaud, S., Flegel, V., Fortier, A., Gasteiger, E., Grosdidier, A., Hernandez, C., Ioannidis, V., Kuznetsov, D., Liechti, R., Moretti, S., Mostaguir, K., Redaschi, N., Rossier, G., … Stockinger, H. (2012). ExPASy: SIB bioinformatics resource portal. *Nucleic Acids Research*, *40*(W1). https://doi.org/10.1093/nar/gks400

Beringer J. E. (1974). R Factor Transfer in *Rhizobium leguminosarum*. *Microbiology*, *84*(1). https://doi.org/10.1099/00221287-84-1-188

Bernal, P., Allsopp, L. P., Filloux, A., & Llamas, M. A. (2017). The *Pseudomonas putida* T6SS is a plant warden against phytopathogens. *ISME Journal*, *11*(4), 972–987. https://doi.org/10.1038/ismej.2016.169

Bernal, P., Furniss, R. C. D., Fecht, S., Leung, R. C. Y., Spiga, L., Mavridou, D. A. I., & Filloux, A. (2021). A novel stabilization mechanism for the type VI secretion system sheath. *Proceedings of the National Academy of Sciences*, *118*(7). https://doi.org/10.1073/pnas.2008500118

Bertani, G. (1951). Studies on lysogenesis I. *Journal of Bacteriology*, *62*(3). https://doi.org/10.1128/jb.62.3.293-300.1951

Bladergroen, M. R., Badelt, K., & Spaink, H. P. (2003). Infection-Blocking Genes of a Symbiotic *Rhizobium leguminosarum* Strain That Are Involved in Temperature-Dependent Protein Secretion. *Molecular Plant-Microbe Interactions®*, *16*(1). https://doi.org/10.1094/MPMI.2003.16.1.53

Boratyn, G. M., Camacho, C., Cooper, P. S., Coulouris, G., Fong, A., Ma, N., Madden, T. L., Matten, W. T., McGinnis, S. D., Merezhuk, Y., Raytselis, Y., Sayers, E. W., Tao, T., Ye, J., & Zaretskaya, I. (2013). BLAST: a more efficient report with usability improvements. *Nucleic Acids Research*, *41*(W1). https://doi.org/10.1093/nar/gkt282

Boyer, F., Fichant, G., Berthod, J., Vandenbrouck, Y., & Attree, I. (2009). Dissecting the bacterial type VI secretion system by a genome wide *in silico* analysis: what can be learned from available microbial genomic resources? *BMC Genomics*, *10*(1). https://doi.org/10.1186/1471-2164-10-104

Cascales, E., & Cambillau, C. (2012). Structural biology of type VI secretion systems. *Philosophical Transactions of the Royal Society B: Biological Sciences*, *367*(1592). https://doi.org/10.1098/rstb.2011.0209

Cherrak, Y., Rapisarda, C., Pellarin, R., Bouvier, G., Bardiaux, B., Allain, F., Malosse, C., Rey, M., Chamot-Rooke, J., Cascales, E., Fronzes, R., & Durand, E. (2018). Biogenesis and structure of a type VI secretion baseplate. *Nature Microbiology*, *3*(12). https://doi.org/10.1038/s41564-018-0260-1

Coutte, L., Antoine, R., Drobecq, H., Locht, C., & Jacob-Dubuisson, F. (2001). Subtilisin-like autotransporter serves as maturation protease in a bacterial secretion pathway. *The EMBO Journal*, *20*(18). https://doi.org/10.1093/emboj/20.18.5040

de Campos, S. B., Lardi, M., Gandolfi, A., Eberl, L., & Pessi, G. (2017). Mutations in Two *Paraburkholderia phymatum* Type VI Secretion Systems Cause Reduced Fitness in Interbacterial Competition. *Frontiers in Microbiology*, *8*. https://doi.org/10.3389/fmicb.2017.02473

de Maagd, R. A., Wijffelman, C. A., Pees, E., & Lugtenberg, B. J. (1988). Detection and subcellular localization of two Sym plasmid-dependent proteins of *Rhizobium leguminosarum* biovar viciae. *Journal of Bacteriology*, *170*(9). https://doi.org/10.1128/jb.170.9.4424-4427.1988

Durand, E., Cambillau, C., Cascales, E., & Journet, L. (2014). VgrG, Tae, Tle, and beyond: the versatile arsenal of Type VI secretion effectors. *Trends in Microbiology*, *22*(9). https://doi.org/10.1016/j.tim.2014.06.004

Figurski, D. H., & Helinski, D. R. (1979). Replication of an origin-containing derivative of plasmid RK2 dependent on a plasmid function provided in trans. *Proceedings of the National Academy of Sciences*, *76*(4). https://doi.org/10.1073/pnas.76.4.1648

Finn, R. D., Coggill, P., Eberhardt, R. Y., Eddy, S. R., Mistry, J., Mitchell, A. L., Potter, S. C., Punta, M., Qureshi, M., Sangrador-Vegas, A., Salazar, G. A., Tate, J., & Bateman, A. (2016). The Pfam protein families database: towards a more sustainable future. *Nucleic Acids Research*, *44*(D1). https://doi.org/10.1093/nar/gkv1344

Jiménez-Guerrero, I., Acosta-Jurado, S., del Cerro, P., Navarro-Gómez, P., López-Baena, F. J., Ollero, F. J., Vinardell, J. M., & Pérez-Montaño, F. (2018). Transcriptomic studies of the effect of nod gene-inducing molecules in rhizobia: Different weapons, one purpose. In *Genes* (Vol. 9, Issue 1). MDPI AG. https://doi.org/10.3390/genes9010001

Jiménez-Guerrero, I., Pérez-Montaño, F., Medina, C., Ollero, F. J., & López-Baena, F. J. (2015). NopC is a rhizobium-specific type 3 secretion system effector secreted by *Sinorhizobium* (*ensifer*) *fredii* HH103. *PLoS ONE*, *10*(11). https://doi.org/10.1371/journal.pone.0142866

Kelley, L. A., Mezulis, S., Yates, C. M., Wass, M. N., & Sternberg, M. J. E. (2015). The Phyre2 web portal for protein modeling, prediction and analysis. *Nature Protocols*, *10*(6). https://doi.org/10.1038/nprot.2015.053

Krogh, A., Larsson, B., von Heijne, G., & Sonnhammer, E. L. L. (2001). Predicting transmembrane protein topology with a hidden markov model: application to complete genomes11Edited by F. Cohen. *Journal of Molecular Biology*, *305*(3). https://doi.org/10.1006/jmbi.2000.4315

Kumar, S., Stecher, G., & Tamura, K. (2016). MEGA7: Molecular Evolutionary Genetics Analysis Version 7.0 for Bigger Datasets. *Molecular Biology and Evolution*, *33*(7). https://doi.org/10.1093/molbev/msw054

Lamrabet, Y., Bellogín, R. A., Cubo, T., Espuny, R., Gil, A., Krishnan, H. B., Megias, M., Ollero, F. J., Pueppke, S. G., Ruiz-Sainz, J. E., Spaink, H. P., Tejero-Mateo, P., Thomas-Oates, J., & Vinardell, J. M. (1999). Mutation in GDP-Fucose Synthesis Genes of *Sinorhizobium fredii* Alters Nod Factors and Significantly Decreases Competitiveness to Nodulate Soybeans. *Molecular Plant-Microbe Interactions®*, *12*(3). https://doi.org/10.1094/MPMI.1999.12.3.207

Le, S. Q., Lartillot, N., & Gascuel, O. (2008). Phylogenetic mixture models for proteins. *Philosophical Transactions of the Royal Society B: Biological Sciences*, *363*(1512). https://doi.org/10.1098/rstb.2008.0180

Letunic, I., & Bork, P. (2016). Interactive tree of life (iTOL) v3: an online tool for the display and annotation of phylogenetic and other trees. *Nucleic Acids Research*, *44*(W1). https://doi.org/10.1093/nar/gkw290

Letunic, I., Doerks, T., & Bork, P. (2015). SMART: recent updates, new developments and status in 2015. *Nucleic Acids Research*, *43*(D1). https://doi.org/10.1093/nar/gku949

Lien, Y.-W., & Lai, E.-M. (2017). Type VI Secretion Effectors: Methodologies and Biology. *Frontiers in Cellular and Infection Microbiology*, *7*. https://doi.org/10.3389/fcimb.2017.00254

Lin, H.-H., Huang, H.-M., Yu, M., Lai, E.-M., Chien, H.-L., & Liu, C.-T. (2018). Functional Exploration of the Bacterial Type VI Secretion System in Mutualism: *Azorhizobium caulinodans* ORS571– *Sesbania rostrata* as a Research Model. *Molecular Plant-Microbe Interactions®*, *31*(8). https://doi.org/10.1094/MPMI-01-18-0026-R

Lin, J.-S., Pissaridou, P., Wu, H.-H., Tsai, M.-D., Filloux, A., & Lai, E.-M. (2018). TagF-mediated repression of bacterial type VI secretion systems involves a direct interaction with the cytoplasmic protein Fha. *Journal of Biological Chemistry*, *293*(23). https://doi.org/10.1074/jbc.RA117.001618

López-Baena, F. J., Monreal, J. A., Pérez-Montaño, F., Guasch-Vidal, B., Bellogín, R. A., Vinardell, J. M., & Ollero, F. J. (2009). The Absence of Nops Secretion in *Sinorhizobium fredii* HH103 Increases *GmPR1* Expression in Williams Soybean. *Molecular Plant-Microbe Interactions®*, *22*(11). https://doi.org/10.1094/MPMI-22-11-1445

López-Baena, F., Ruiz-Sainz, J., Rodríguez-Carvajal, M., & Vinardell, J. (2016). Bacterial Molecular Signals in the *Sinorhizobium fredii*-Soybean Symbiosis. *International Journal of Molecular Sciences*, *17*(5). https://doi.org/10.3390/ijms17050755

Martinelli, F., Ollero, F. J., Giovino, A., Perrone, A., Bekki, A., Sikora, S., el Nabbout, R., Bouhadida, M., Yucel, D., Bazzicalupo, M., Mengoni, A., & Pérez-Montaño, F. (2020). Proposed research for innovative solutions for chickpeas and beans in a climate change scenario: The Mediterranean basin. *Sustainability (Switzerland)*, *12*(4). https://doi.org/10.3390/su12041315

Miller, J. H. (1972). *Experiment in molecular genetics*. Cold Spring Harbor Laboratory.

Mougous, J. D. (2006). A Virulence Locus of *Pseudomonas aeruginosa* Encodes a Protein Secretion Apparatus. *Science*, *312*(5779). https://doi.org/10.1126/science.1128393

Mougous, J. D., Gifford, C. A., Ramsdell, T. L., & Mekalanos, J. J. (2007). Threonine phosphorylation post-translationally regulates protein secretion in *Pseudomonas aeruginosa*. *Nature Cell Biology*, *9*(7). https://doi.org/10.1038/ncb1605

Nelson, M. S., & Sadowsky, M. J. (2015). Secretion systems and signal exchange between nitrogen-fixing rhizobia and legumes. *Frontiers in Plant Science*, *6*. https://doi.org/10.3389/fpls.2015.00491

Oldroyd, G. E. D., & Downie, J. A. (2008). Coordinating Nodule Morphogenesis with Rhizobial Infection in Legumes. *Annual Review of Plant Biology*, *59*(1). https://doi.org/10.1146/annurev.arplant.59.032607.092839

Oldroyd, G. E. D., Murray, J. D., Poole, P. S., & Downie, J. A. (2011). The Rules of Engagement in the Legume-Rhizobial Symbiosis. *Annual Review of Genetics*, *45*(1). https://doi.org/10.1146/annurev-genet-110410-132549

Pérez-Montaño, F., Alías-Villegas, C., Bellogín, R. A., del Cerro, P., Espuny, M. R., Jiménez-Guerrero, I., López-Baena, F. J., Ollero, F. J., & Cubo, T. (2014). Plant growth promotion in cereal and leguminous agricultural important plants: From microorganism capacities to crop production. In *Microbiological Research* (Vol. 169, Issues 5–6, pp. 325–336). Urban und Fischer Verlag Jena. https://doi.org/10.1016/j.micres.2013.09.011

Pérez-Montaño, F., Jiménez-Guerrero, I., Acosta-Jurado, S., Navarro-Gómez, P., Ollero, F. J., Ruiz-Sainz, J. E., López-Baena, F. J., & Vinardell, J. M. (2016). A transcriptomic analysis of the effect of genistein on *Sinorhizobium fredii* HH103 reveals novel rhizobial genes putatively involved in symbiosis. *Scientific Reports*, *6*(1). https://doi.org/10.1038/srep31592

Pérez-Montaño, F., Jiménez-Guerrero, I., del Cerro, P., Baena-Ropero, I., López-Baena, F. J., Ollero, F. J., Bellogín, R., Lloret, J., & Espuny, R. (2014). The symbiotic biofilm of *Sinorhizobium fredii* SMH12, necessary for successful colonization and symbiosis of *Glycine max* cv Osumi, is regulated by quorum sensing systems and inducing flavonoids via NodD1. *PLoS ONE*, *9*(8). https://doi.org/10.1371/journal.pone.0105901

Pfaffl, M. W. (2001). A new mathematical model for relative quantification in real-time RT-PCR. *Nucleic Acids Research*, *29*(9). https://doi.org/10.1093/nar/29.9.e45

Pissaridou, P., Allsopp, L. P., Wettstadt, S., Howard, S. A., Mavridou, D. A. I., & Filloux, A. (2018). The *Pseudomonas aeruginosa* T6SS-VgrG1b spike is topped by a PAAR protein eliciting DNA damage to bacterial competitors. *Proceedings of the National Academy of Sciences*, *115*(49). https://doi.org/10.1073/pnas.1814181115

Pueppke, S. G., & Broughton, W. J. (1999). *Rhizobium* sp. Strain NGR234 and *R. fredii* USDA257 Share Exceptionally Broad, Nested Host Ranges. *Molecular Plant-Microbe Interactions®*, *12*(4). https://doi.org/10.1094/MPMI.1999.12.4.293

Pukatzki, S., McAuley, S. B., & Miyata, S. T. (2009). The type VI secretion system: translocation of effectors and effector-domains. In *Current Opinion in Microbiology* (Vol. 12, Issue 1, pp. 11–17). Elsevier Ltd. https://doi.org/10.1016/j.mib.2008.11.010

Salinero-Lanzarote, A., Pacheco-Moreno, A., Domingo-Serrano, L., Durán, D., Ormeño-Orrillo, E., Martínez-Romero, E., Albareda, M., Palacios, J. M., & Rey, L. (2019). The Type VI secretion system of *Rhizobium etli* Mim1 has a positive effect in symbiosis. *FEMS Microbiology Ecology*, *95*(5). https://doi.org/10.1093/femsec/fiz054

Sambrook, J., Fritsch, E. F., & Maniatis, T. (1989). *Molecular Cloning. A Laboratory Manual*. Cold Spring Harbor Laboratory Press.

Schäfer, A., Tauch, A., Jäger, W., Kalinowski, J., Thierbach, G., & Pühler, A. (1994). Small mobilizable multi-purpose cloning vectors derived from the *Escherichia coli* plasmids pK18 and pK19: selection of defined deletions in the chromosome of Corynebacterium glutamicum. *Gene*, *145*(1). https://doi.org/10.1016/0378-1119(94)90324-7

Sievers, F., Wilm, A., Dineen, D., Gibson, T. J., Karplus, K., Li, W., Lopez, R., McWilliam, H., Remmert, M., Söding, J., Thompson, J. D., & Higgins, D. G. (2011). Fast, scalable generation of high-quality protein multiple sequence alignments using Clustal Omega. *Molecular Systems Biology*, *7*(1). https://doi.org/10.1038/msb.2011.75

Silverman, J. M., Brunet, Y. R., Cascales, E., & Mougous, J. D. (2012). Structure and Regulation of the Type VI Secretion System. *Annual Review of Microbiology*, *66*(1). https://doi.org/10.1146/annurev-micro-121809-151619

Simon, R. (1984). High frequency mobilization of gram-negative bacterial replicons by the in vitro constructed Tn5-Mob transposon. *Molecular and General Genetics MGG*, *196*(3). https://doi.org/10.1007/BF00436188

Spaink, H. P., Okker, R. J. H., Wijffelman, C. A., Pees, E., & Lugtenberg, B. J. J. (1987). Promoters in the nodulation region of the *Rhizobium leguminosarum* Sym plasmid pRL1JI. *Plant Molecular Biology*, *9*(1). https://doi.org/10.1007/BF00017984

Staehelin, C., & Krishnan, H. B. (2015). Nodulation outer proteins: double-edged swords of symbiotic rhizobia. *Biochemical Journal*, *470*(3). https://doi.org/10.1042/BJ20150518

Sullivan, M. J., Petty, N. K., & Beatson, S. A. (2011). Easyfig: a genome comparison visualizer. *Bioinformatics*, *27*(7). https://doi.org/10.1093/bioinformatics/btr039

Vincent, J. M. (1970). The modified Fåhraeus slide technique. In *A Manual for the Practical Study of Root Nodule Bacteria* (pp. 144–145). Blackwell Scientific Publications.

Walker, T. S., Bais, H. P., Grotewold, E., & Vivanco, J. M. (2003). Root Exudation and Rhizosphere Biology. *Plant Physiology*, *132*(1). https://doi.org/10.1104/pp.102.019661

Yu, N. Y., Wagner, J. R., Laird, M. R., Melli, G., Rey, S., Lo, R., Dao, P., Sahinalp, S. C., Ester, M., Foster, L. J., & Brinkman, F. S. L. (2010). PSORTb 3.0: improved protein subcellular localization prediction with refined localization subcategories and predictive capabilities for all prokaryotes. *Bioinformatics*, *26*(13). https://doi.org/10.1093/bioinformatics/btq249

Zaat, S. A., Wijffelman, C. A., Spaink, H. P., van Brussel, A. A., Okker, R. J., & Lugtenberg, B. J. (1987). Induction of the *nodA* promoter of *Rhizobium leguminosarum* Sym plasmid pRL1JI by plant flavanones and flavones. *Journal of Bacteriology*, *169*(1). https://doi.org/10.1128/jb.169.1.198-204.1987